Polymer 53 (2012) 5754–5759

Contents lists available at SciVerse ScienceDirect

Polymer

journal homepage: www.elsevier.com/locate/polymer

Top–down meets bottom–up: A comparison of the mechanical properties of melt electrospun and self-assembled 1,3,5-benzenetrisamide fibers

Daniel Kluge [a,1,2], Julia. C. Singer [b,2], Benedikt R. Neugirg [a,1], Jens W. Neubauer [a,1], Hans-Werner Schmidt [b], Andreas Fery [a,*]

[a] Physical Chemistry II and Bayreuth Center for Colloids and Interfaces, University of Bayreuth, Universitaetsstrasse 30, D-95440 Bayreuth, Germany
[b] Macromolecular Chemistry I, Bayreuth Institute of Macromolecular Research and Bayreuth Center for Colloids and Interfaces, University of Bayreuth, Universitaetsstrasse 30, D-95440 Bayreuth, Germany

ARTICLE INFO

Article history:
Received 31 August 2012
Received in revised form
5 October 2012
Accepted 6 October 2012
Available online 12 October 2012

Keywords:
1,3,5-Benzenetrisamides
Melt electrospinning
Self-assembly

ABSTRACT

1,3,5-Benzenetrisamides (BTAs) are a prominent class of low-molecular weight compounds in supramolecular chemistry. They are well-known to self-assemble into micro- and nanofibers in a bottom–up approach. At the same time, BTAs are also suitable for top-down processing by melt electrospinning. In this work, we demonstrate for the first time that both approaches lead to mechanically robust BTA fibers. We compare self-assembled and electrospun fibers of N,N,N″-tripropyl-1,3,5-benzenetricarboxamide on multiple length scales. X-ray diffraction (XRD) reveals the same crystal structure independently from the preparation method. Using scanning electron microscopy (SEM), we observe significantly different morphologies of both fiber types on the sub-micron-scale. However, atomic force microscopy (AFM) bending experiments show that despite differences in morphology, Young's modulus is comparable for both types and in the lower GPa range (3–5 GPa). Thus, both top–down and bottom–up techniques with their complementary features in terms of accessible structures and potential applications are available for this class of materials.

1. Introduction

The controlled fabrication of well-defined microscopic fibrillar structures has become one of the main topics in materials science [1–3]. Networks and nonwovens based on these structures possess exceptional properties, such as high surface area, possibility for easy functionalization and superior mechanical strength [4]. These are promising features for applications such as tissue engineering, drug delivery, sensors, micro-/nanoelectromechanical systems (MEMS/NEMS), and filtration [3–7]. Especially fibers of sub-micron or nanoscale diameters are of interest due to their surface to volume ratio and the possibility to form structures with small mesh-sizes. Two approaches are feasible to access these length scales: Bottom–up approaches rely on the self-assembly of smaller units (even single molecules) to hierarchical structures [8,9]. Top–down approaches, such as electrospinning, shape the materials directly into the desired structure. Especially for fibers and nonwovens, a great variety of structures has been demonstrated [10].

Both techniques are complementary in various ways: Since self-assembly allows simultaneous formation and growth of many fibers in a given volume, it is preferable in terms of processing times, especially for upscaling. In addition, if the processing conditions are chosen well, smaller fiber diameters are accessible in a more simple fashion than in electrospinning [9,11]. On the downside, self-assembled fibers have smaller length and random orientation since they grow from many nuclei.

The advantage of electrospinning is that fibers can easily be formed with macroscopic length and well-defined orientation on macroscopic length scales. This even allows the controlled formation of superstructures at the micrometer level and above. However, the processing times are longer since electrospinning is a sequential process, in which the time necessary to form fibers is proportional to the total fiber length.

To offer the highest flexibility, it would be desirable to switch from one to the other approach for the same class of materials – especially for the formation of hierarchically organized structures which span multiple length scales.

* Corresponding author. Tel.: +49 921 55 27 51; fax: +49 921 55 20 59.
E-mail addresses: hans-werner.schmidt@uni-bayreuth.de (H.-W. Schmidt), andreas.fery@uni-bayreuth.de (A. Fery).
[1] Tel.: +49 921 55 27 51; fax: +49 921 55 20 59.
[2] Julia C. Singer and Daniel Kluge contributed equally to this work.

0032-3861/$ – see front matter © 2012 Elsevier Ltd. All rights reserved.
http://dx.doi.org/10.1016/j.polymer.2012.10.016

Lately, the self-assembly of 1,3,5-benzenetrisamides (BTAs) into fibrillar structures has attracted increasing research interest [12,13]. The benzene core realizes a planar and symmetric moiety and three amide groups allow the formation of strong hydrogen bonds between adjacent molecules resulting in supramolecular architectures [14]. BTAs are well-known as nucleating agents for polyvinylidene fluoride and polypropylene [15–18]. Moreover, they are applied as organo- and hydrogelators [19–22], as additives to improve the charge storage capability of electret materials [23] and as supramolecular materials [24,25].

In addition to their bottom–up properties, we recently reported on the melt electrospinning of various BTAs and 1,3,5-cyclohexanetrisamides into defined fine fibers with a narrow size distribution [26]. Although a high molecular mass polymer is not essential for obtaining uniform electrospun fibers [27], electrospinning of low molecular weight substances is still unusual. BTAs form macrodipoles along the main axis of the column during the supramolecular assembly process within external electric fields and consequently offer excellent pre-conditions for electrospinning [28–30]. The melt electrospinning of BTAs is an exciting new top–down approach for self-assembling systems. It offers the possibility to overcome the strict limitation of the self-assembly conditions and consequently opens up a wide field of new applications for BTAs.

For all applications, a reasonable mechanical stability is an essential prerequisite. However, regardless by which means the BTA fibers are prepared, the mechanical characterization on a micron- or sub-micron scale requires sophisticated methods. A powerful technique is nanomechanical bending experiments, which have been used for the mechanical investigation of polymer nanofibers [31–33], biological materials [34–38], CNTs [39,40], and nanowires [41–43]. In previous studies, we performed bending experiments on BTA micro- and nanofibers obtained via controlled self-assembly from nonpolar solvents. The experiments demonstrated that their molecular architecture allows control over the fiber morphology without decreasing their mechanical stability [44,45].

In this work, we address the question whether the properties of BTA fibers are affected by using a top–down approach instead of a bottom–up approach. For that purpose, we prepare fibers of the same 1,3,5-benzenetrisamide via self-assembly from solution and melt electrospinning. This allows us for the first time to compare crystal structure, morphology and nano-mechanical properties of BTA fibers prepared from the same material.

2. Results and discussion

For the comparison, we prepared fibers of N,N′,N″-tripropyl-1,3,5-benzenetricarboxamide **1** (Scheme 1) via bottom–up (in the following termed SA-fibers) as well as top–down techniques (in the following termed ES-fibers). The SA-fibers were produced via controlled self-assembly by cooling of a solution of **1** in 2,2,4,4,6,8,8-heptamethylnonane (HMN). As top–down approach, we used melt electrospinning.

In order to investigate structural features on the Ångström-scale, we performed XRD measurements on chopped fibers. The X-ray diffractograms of both systems are identical, indicating the same crystal structure (Fig. 1, see also Supplementary material S1). The peaks of the SA fibers show a narrower full width at half maximum, what is expected since a higher degree of crystallinity is typically achieved by the bottom–up process. Due to hydrogen bonds, **1** packs in a primitive cubic [4^6]-pcu supramolecular three-dimensional network. The molecules are located in planes, which are stacked along the c axis [46]. While it is on first glance surprising that the electrospun material shows an as well-developed crystalline order as the self-assembled material, we demonstrated in previous work that ES-fibers are not formed from a molecular liquid state but from a melt which still consists of short columnar pre-aggregates [26,47]. Thus the crystallization process is greatly accelerated due to the pre-aggregation of single molecules and leads to a poly-crystalline state.

The microscopic morphology of the fibers was investigated via SEM. The average diameter of the SA- and ES-fibers, respectively, was 1.2 ± 0.7 μm and 0.8 ± 0.2 μm (size distribution diagrams see S2 and S3). Although the diameters of SA- and ES-fibers are comparable, the morphology of both systems shows significant differences. SA-fibers possess a hierarchical structure: they consist of bundles of individual strands that have an average diameter of about 100 nm (see inset of Fig. 2, top, left). This bundle substructure is also visible in the irregular fracture sections of the SA-fibers (Fig. 2, top, right). In contrast, ES-fibers exhibit a homogenous, smooth surface without defects or pronounced surface features (Fig. 2, bottom, left). Even fracture sections of the ES-fibers are very smooth without any detailed sub-structure or obvious defects (Fig. 2, bottom, right).

These differences in the microscopic morphology arise from the significantly different methods used to generate the two investigated fiber types. The crystallization process of the SA-fibers is much slower, allowing the development of larger crystals which then bundle into fibers. This explains the broader diameter distribution found for SA-fibers. In contrast, during electrospinning, ES-fibers are obtained from molten material, resulting in a homogenous strand.

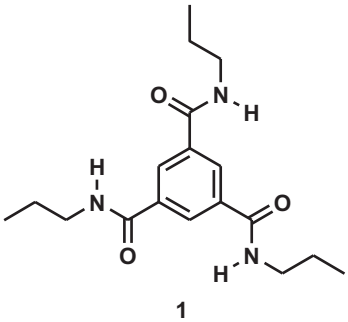

1

Scheme 1. Chemical structure of N,N′,N″-tripropyl-1,3,5-benzenetricarboxamide (**1**).

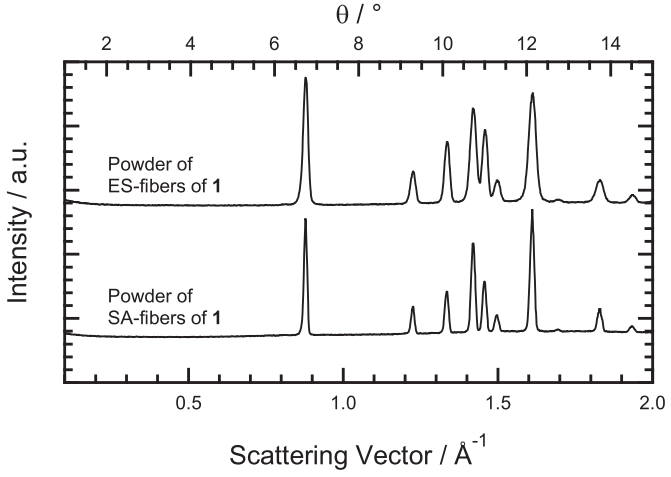

Fig. 1. X-ray diffractograms of SA- and ES-fibers in powder form.

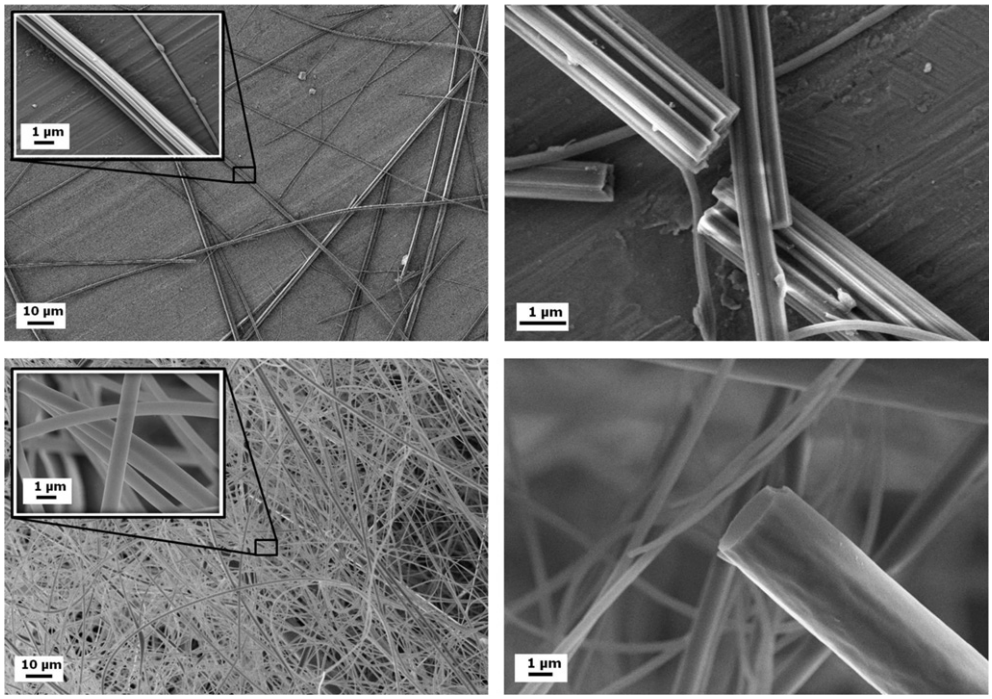

Fig. 2. Top: SEM micrograph of the SA-fibers (left) and of a fracture section (right). Bottom: SEM micrograph of the ES-fibers of **1** (left) and of a fracture section (right). More detailed structures of the fibers are shown in the insets.

In order to evaluate the mechanical properties of both systems, we performed nanomechanical bending experiments using an atomic force microscope (AFM). A detailed description of the theoretical background and experimental procedures can be found elsewhere [44]. Both fiber types were transferred to micro-structured glass substrates (Fig. 3) to achieve a free-standing configuration (Fig. 4a). In this configuration, no deformation was observed when applying a vertical load to the segments supported by the substrate (Fig. 4b). Therefore, only bending deformations are measured when applying a load to the free-standing segments over the gap and the results can be evaluated with classical beam theory [48].

We recorded stiffness profiles by measuring the stiffness $k(x)$ at several positions x along the free-standing segment (Fig. 4c) and calculated Young's modulus E of each investigated segment by fitting the profiles with the double-clamped beam model (Equation (1)) [42,44,48].

$$k(x) = \frac{3L^3EI}{(L-x)^3x^3} \tag{1}$$

Here, L is the length of the free-standing segment and I is the area moment of inertia. We imaged each investigated sample with the AFM to obtain the correct fiber thickness and shape to avoid errors as I shows quartic scaling with the radius.

Since Young's modulus is a material property, it is possible to normalize the profiles of all investigated SA- and ES-fibers, respectively, to calculate the averaged values [45]. The resulting Young's moduli were $E_{SA} = 3.6 \pm 0.4$ GPa and $E_{ES} = 4.7 \pm 0.6$ GPa (see S4 for more detailed data). In addition, we calculated the modulus of each fiber individually and determined the distributions (Fig. 4d). While the ES-fibers show a slightly higher average modulus than the SA-fibers, the distributions are similar for both systems. We also investigated if shearing affects the measurements, but found no influence (see S5).

Our experiments show that the moduli of SA- and ES-fibers are in the same range and comparable to those of (semi) crystalline or glassy polymers like PVC and PMMA, common fiber materials like nylon and electrospun collagen fibers [33,49]. The elastic properties of the fibers are also in good agreement with BTAs with different molecular structure where Young's moduli between 2 and 4 GPa have been observed [44,45]. In order to understand the mechanical similarity of these morphologically quite different SA- and ES-fibers, one has to look at the underlying principles behind the mechanics. In both systems, intermolecular hydrogen bonds and π-

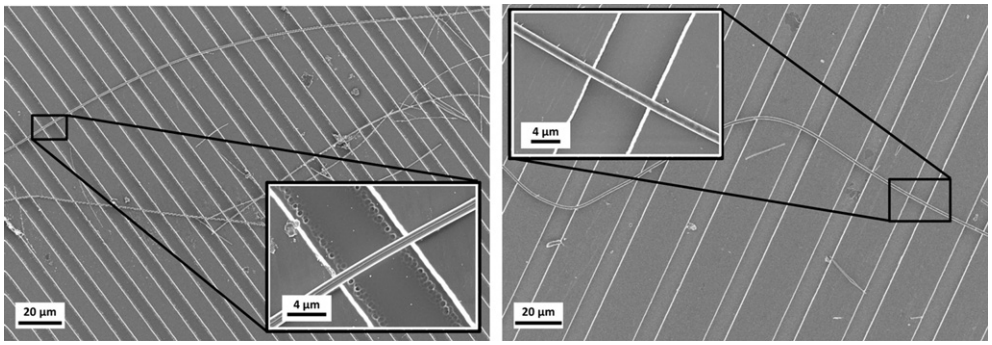

Fig. 3. SA-fibers (left) and ES-fibers (right) on micro structured glass substrates for AFM bending experiments.

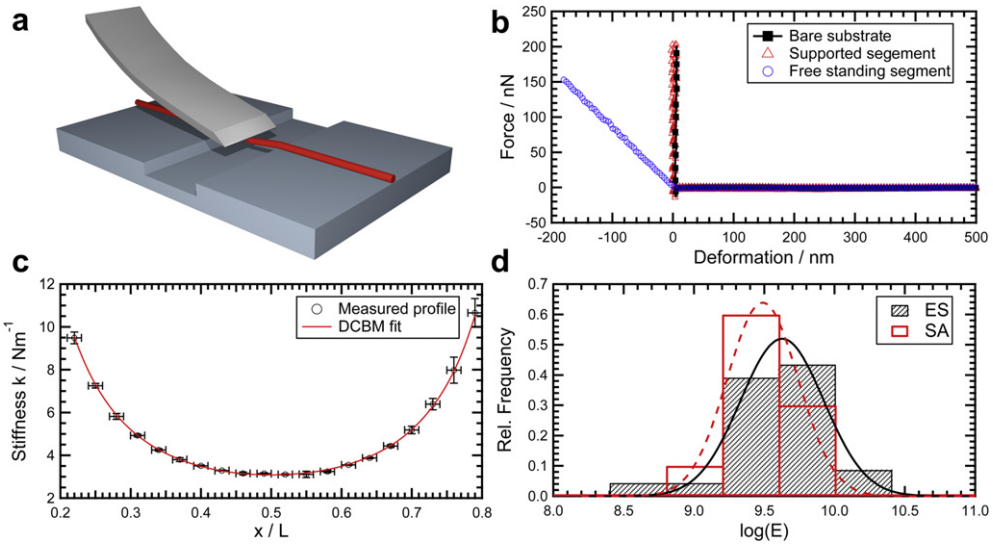

Fig. 4. a) Schematic setup of the bending experiments. b) Force-deformation measurements on bare glass substrates (black squares), substrate-supported (red triangles) and free-standing segments (blue circles) of ES-fibers. c) Stiffness profile of a free-standing ES-fiber segment fitted with the DCBM. d) Distribution of the Young's moduli of SA-fibers (open bars, dashed line) and ES-fibers (hatched bars, solid line). (For interpretation of the references to color in this figure legend, the reader is referred to the web version of this article.)

stacking are responsible for the formation and cohesion of the fibers. Likewise, the ensemble of these noncovalent interactions determines the response to mechanical stresses. Therefore, despite differences in their morphology, it is reasonable that SA- and ES-fibers posses comparable elastic properties. Although the distributions of the moduli are rather broad, we observed a tendency toward a slightly lower modulus of the SA-fibers compared to the ES-fibers. This can be explained by their bundle-substructure which is more likely prone to defects. However, the effect is small and within the range of sample deviations and the error of the measurements. The important finding is that both fiber types show a remarkable mechanical stability despite the small molecule size and the absence of covalent interactions.

3. Conclusions

In this study we demonstrated for the first time that mechanically robust BTA fibers can be accessed via bottom–up- and top–down-approaches. We prepared self-assembled (SA) and melt electrospun (ES) fibers from the same compound **1** and obtained fibers with an average diameter of 1.2 ± 0.7 μm and 0.8 ± 0.2 μm for SA- and ES-fibers, respectively. On the Ångström-scale, XRD measurements show the same crystal structure of the fibers, independently of the preparation method. On the microscopic scale, SEM measurements however clearly revealed morphological differences: The self-assembled fibers possessed a hierarchical structure, consisting of firmly connected bundles of individual strands, while melt electrospun fibers showed a smooth and homogenous structure. AFM bending experiments, which probe the mechanical behavior on the length scale of the whole assembly, revealed that Young's modulus E was not significantly affected by changing the preparation process. While the order of magnitude and distributions of the moduli were comparable, the average values suggested that E_{SA} (3.6 ± 0.4 GPa) was slightly lower than E_{ES} (4.7 ± 0.6 GPa) due to the bundle-substructure of the SA-fibers which is more likely prone to defects. However, the difference was small and within the error range of measurements. Still, our results prove that mechanically robust BTA fibers can be obtained by bottom–up as well as top–down approaches.

These findings open interesting perspectives for structure formation from BTAs. First, the relatively high elastic constants in the lower GPa range that are found for both approaches demonstrate that the fibrillar structures are mechanically robust regardless of how they are formed, qualifying them as a platform for hierarchical structure formation. Second, the results show that BTAs are shapeable into fibers with both approaches. This is interesting, since bottom–up and top–down approaches have complementary advantages and disadvantages, as discussed in the introduction. Now with this system, the best of the bottom–up and top–down approaches can be combined for one materials class and used for creating hierarchically structured nonwovens for example for filter applications.

4. Experimental section

4.1. Material

N,N′,N″-tripropyl-1,3,5-benzenetricarboxamide **1** was synthesized according to the literature [50]. The melting temperature of **1** is 289 °C and was determined in a Perkin Elmer Diamond DSC (heating rate: 10 K/min, nitrogen flow: 20 mL/min). The temperature at a 10% weight loss is 351 °C. The measurement was performed in a Mettler SDTA 851 TGA at 10 K/min (nitrogen flow: 60 mL/min). Isothermal TGA runs at the spinning temperature (290 °C) under nitrogen atmosphere were performed to verify the thermal stability of **1** during the period of the electrospinning process. **1** shows a weight loss below 5 wt.% for 55 min.

4.2. SA-fiber preparation

In 2,2,4,4,6,8,8-heptamethylnonane (HMN) 600 ppm of **1** were dissolved under reflux at 240 °C and cooled to room temperature. To ensure a controlled self-assembly behavior, 200 μL of the suspension were heated in a custom designed high pressure pan to 240 °C for 10 min in the Dropping Point Cell FP83HT from METTLER TOLEDO followed by cooling to 30 °C with 5 K/min (controlled with the METTLER TOLEDO Central Processor FP90). For the bending experiments, identical structured glass substrates were wetted

with 10 μL of blank HMN, 0.5 μL of the fiber suspension were added and the samples were allowed to dry overnight.

4.3. ES-fiber preparation

The melt electrospinning experiments were carried out as described elsewhere [26]. **1** was equilibrated in a syringe with an inner needle diameter of 0.6 mm for 3 min at its melting point at 290 °C (temperature of the heated cylinder around the syringe body in the melt electrospinning set-up) before applying high voltage of −30 kV. The distance between needle tip and collector was 6 cm and the feeding rate 500 μL/h. The electrospun material was collected on a single 12 mm diameter aluminum SEM stub with a carbon tab which was mounted on top of the collector plate. The melt electrospinning experiment was carried out during 15 min. For the bending experiments, the fibers were transferred to structured glass substrates (GeSiM GmbH, Grosserkmannsdorf, Germany; channel widths 20, 30 and 40 μm, respectively) by gently bringing the SEM stub and the substrates in contact.

4.4. XRD-measurements

The XRD-measurements in the angle range of $\theta = 0.5°–15°$ were carried out on a Huber Guinier diffractometer 600. To get Cu $K_{\alpha 1}$ radiation ($\lambda = 154.051$ pm) it is equipped with a Huber germanium monochromator 61. An extra slit diaphragm reduces the broadening of the primary beam due to scattering in air. The samples were prepared in soda glass capillaries (1.5–2 mm diameter) from powder.

4.5. Scanning electron microscopy

For preparation of the SA-fiber SEM samples, 5 μL of the HMN-suspension was put in aluminum pans and the solvent was evaporated under reduced pressure. ES-fibers of **1** were directly spun onto a SEM specimen stub with a carbon tab. All samples were sputtered with platinum (2.0 nm) in a Cressington sputter coater 208HR. The SEM micrographs were recorded on a Zeiss ULTRA plus FESEM (Zeiss, Jena, Germany). To obtain a reliable size distribution, 250 individual SA- and ES-fibers, respectively, were evaluated using AxioVision LE Software (Carl Zeiss AG, Germany). The histograms can be found in the Supplementary material S2 and S3.

4.6. AFM measurements

All AFM measurements were performed on a Nanowizard I (JPK Instruments AG, Berlin, Germany). The bending experiments were performed as previously reported [44]. Details about the used cantilever types and applied loads can be found in the Supplementary material S6.

Acknowledgments

This work received financial support from the German Research Foundation (Deutsche Forschungsgemeinschaft) within the SFB 840, project B8. We thank Doris Hanft for help with the synthesis of the 1,3,5-benzenetrisamide, Martina Heider and Dr. Beate Förster from Bayreuth Institute of Macromolecular Research for support with the SEM images and Andreas Timme and Marina Behr for the XRD measurements. DK, JCS, BRN and JWN acknowledge the support of the Elite Network of Bavaria.

Appendix A. Supplementary data

Supplementary data related to this article can be found, in the online version, at http://dx.doi.org/10.1016/j.polymer.2012.10.016.

References

[1] Xia YN, Yang PD, Sun YG, Wu YY, Mayers B, Gates B, et al. Advanced Materials 2003;15(5):353–89.
[2] Kuttner C, Tebbe M, Schlaad H, Burgert I, Fery A. ACS Applied Materials & Interfaces 2012;4:3485–92.
[3] Agarwal S, Wendorff JH, Greiner A. Polymer 2008;49(26):5603–21.
[4] Jayaraman K, Kotaki M, Zhang YZ, Mo XM, Ramakrishna S. Journal of Nanoscience and Nanotechnology 2004;4(1–2):52–65.
[5] Moriarty P. Reports on Progress in Physics 2001;64(3):297–381.
[6] Barhate RS, Ramakrishna S. Journal of Membrane Science 2007;296(1–2):1–8.
[7] Lutolf MP, Hubbell JA. Nature Biotechnology 2005;23(1):47–55.
[8] Palmer LC, Stupp SI. Accounts of Chemical Research 2008;41(12):1674–84.
[9] Kimizuka N. Self-assembly of supramolecular nanofibers. In: Shimizu T, editor. Self-assembled nanomaterials I: nanofibers, vol. 219. Berlin: Springer-Verlag Berlin; 2008. p. 1–26.
[10] Greiner A, Wendorff JH. Angewandte Chemie-International Edition 2007;46(30):5670–703.
[11] Hutmacher DW, Dalton PD. Chemistry-an Asian Journal 2011;6(1):44–56.
[12] Filot IAW, Palmans ARA, Hilbers PAJ, van Santen RA, Pidko EA, Greef TFA. The Journal of Physical Chemistry B 2010;114(43):13667–74.
[13] Kristiansen M, Smith P, Chanzy H, Baerlocher C, Gramlich V, McCusker L, et al. Crystal Growth & Design 2009;9(6):2556–8.
[14] Lightfoot MP, Mair FS, Pritchard RG, Warren JE. Chemical Communications 1945–1946;1999(19).
[15] Abraham F, Schmidt H-W. Polymer 2010;51(4):913–21.
[16] Abraham F, Ganzleben S, Hanft D, Smith P, Schmidt H-W. Macromolecular Chemistry & Physics 2010;211:171–81.
[17] Blomenhofer M, Ganzleben S, Hanft D, Schmidt H-W, Kristiansen M, Smith P, et al. Macromolecules 2005;38(9):3688–95.
[18] Schmidt M, Wittmann JJ, Kress R, Schneider D, Steuernagel S, Schmidt HW, et al. Crystal Growth & Design 2012;12(5):2543–51.
[19] Yasuda Y, Iishi E, Inada H, Shirota Y. Chemistry Letters 1996;7:575–6.
[20] Hanabusa K, Koto C, Kimura M, Shirai H, Kakehi A. Chemistry Letters 1997;5:429–30.
[21] Kumar DK, Jose DA, Dastidar P, Das A. Chemistry of Materials 2004;16(12):2332–5.
[22] Bernet A, Behr M, Schmidt H-W. Soft Matter 2011;7(3):1058.
[23] Mohmeyer N, Behrendt N, Zhang X, Smith P, Altstädt V, Sessler GM, et al. Polymer 2007;48(6):1612–9.
[24] Roosma J, Mes T, Leclere P, Palmans ARA, Meijer EW. Journal of the American Chemical Society 2008;130(4):1120–1.
[25] Mes T, Smulders MMJ, Palmans ARA, Meijer EW. Macromolecules 2010;43(4):1981–91.
[26] Singer JC, Giesa R, Schmidt H-W. Soft Matter 2012;8:9972–6.
[27] Hunley MT, McKee MG, Gupta P, Wilkes GL, Long TE. MRS Proceedings 2006;948.
[28] Sakamoto A, Ogata D, Shikata T, Urakawa O, Hanabusa K. Polymer 2006;47(4):956–60.
[29] Tomatsu I, Fitié CFC, Byelov D, Jeu WH, Magusin PCMM, Wübbenhorst M, et al. The Journal of Physical Chemistry B 2009;113(43):14158–64.
[30] Kulkarni C, Reddy SK, George SJ, Balasubramanian S. Chemical Physics Letters 2011;515(4–6):226–30.
[31] Tan EPS, Lim CT. Applied Physics Letters 2004;84(9):1603–5.
[32] Shin MK, Kim SI, Kim SJ, Kim S-K, Lee H. Applied Physics Letters 2006;88(19):193901–3.
[33] Yang L, Fitie CFC, van der Werf KO, Bennink ML, Dijkstra PJ, Feijen J. Biomaterials 2008;29(8):955–62.
[34] Xu W, Mulhern PJ, Blackford BL, Jericho MH, Templeton I. Scanning Microscopy 1994;8(3):499–506.
[35] Kis A, Kasas S, Babic B, Kulik AJ, Benoit W, Briggs GAD, et al. Physical Review Letters 2002;89(24):4.
[36] Guzman C, Jeney S, Kreplak L, Kasas S, Kulik AJ, Aebi U, et al. Journal of Molecular Biology 2006;360(3):623–30.
[37] Orso S, Wegst U, Arzt E. Journal of Materials Science 2006;41(16):5122–6.
[38] Stamov DR, Nguyen TAK, Evans HM, Pfohl T, Werner C, Pompe T. Biomaterials 2011;32(30):7444–53.
[39] Wong EW, Sheehan PE, Lieber CM. Science 1997;277(5334):1971–5.
[40] Salvetat JP, Briggs GAD, Bonard JM, Bacsa RR, Kulik AJ, Stockli T, et al. Physical Review Letters 1999;82(5):944–7.
[41] Wu B, Heidelberg A, Boland JJ. Nature Materials 2005;4:525–9.
[42] Chen YX, Dorgan BL, McIlroy DN, Aston DE. Journal of Applied Physics 2006;100(10):104301.
[43] Zhang H, Tang J, Zhang L, An B, Qin LC. Applied Physics Letters 2008;92(17):3.
[44] Kluge D, Abraham F, Schmidt S, Schmidt HW, Fery A. Langmuir 2010;26(5):3020–3.

[45] Kluge D, Singer JC, Neubauer JW, Abraham F, Schmidt H-W, Fery A. Small 2012;8(16):2563–70.
[46] Jimenez CA, Belmar JB, Ortiz L, Hidalgo P, Fabelo O, Pasan J, et al. Crystal Growth & Design 2009;9(12):4987–9.
[47] Timme A, Kress R, Albuquerque RQ, Schmidt H-W. Chemistry – A European Journal 2012;18(27):8329–39.
[48] Gere JM, Goodno BJ. Mechanics of materials. 7th ed. Toronto: Cengage Learning; 2008.
[49] Brandrup J, Immergut EH, Grulke EA, Abe A, Bloch DR. In: Polymer handbook, vol. 1. Hoboken, New Jersey: John Wiley & Sons, Inc; 1999. p. V/162–7.
[50] Schmidt H-W, Smith P, Blomenhofer M. In: Inc. CSCH, editor. vol. WO 02/46300 A2, 2002.